Progress In Electromagnetics Research, PIER 47, 193–212, 2004

NUMERICAL DISPERSION AND IMPEDANCE ANALYSIS FOR 3D PERFECTLY MATCHED LAYERS USED FOR TRUNCATION OF THE FDTD COMPUTATIONS

W. Yuan and E.-P. Li

Computational Electromagnetics and Electronics Division
Institute of High Performance Computing, Singapore

Abstract—The 3D Berenger's and uniaxial perfectly matched layers used for the truncation of the FDTD computations are theoretically investigated respectively in the discrete space, including numerical dispersion and impedance characteristics. Numerical dispersion for both PMLs is different from that of the FDTD equations in the normal medium due to the introduction of loss. The impedance in 3D homogeneous Berenger's PML medium is the same as that in the truncated normal medium even in the discrete space, however, the impedance in 3D homogenous UPML medium is different, but the discrepancy smoothly changes as the loss in the UPML medium slowly change. Those insights acquired can help to understand why both 3D PMLs can absorb the outgoing wave with arbitrary incidence, polarization, and frequency, but with different efficiency.

1. INTRODUCTION

The relentless advances in VLSI technologies result in significant challenges in electromagnetic modeling for present electronic systems, which has usually been resorted to numerical techniques. The finite-difference time-domain (FDTD) method [1] has come into prominence in full-wave numerical modeling, where one of the greatest challenges is the efficient and accurate solution to unbounded electromagnetic wave interaction problems. Over the years, the techniques on artificial boundary conditions, i.e., Mur's and Liao's absorbing boundary conditions and the technique "superabsorption" [2–4] have been developed. However, those methods are sensitive to frequency and incident angle so that the external boundaries had to be placed a long distance away from the scatterers, leading to prohibitive computational overhead.

Analogous to physical treatment of anechoic chamber, the perfectly matched layers (PML) absorbing boundary condition was developed as an efficient absorber [5–7]. It outperforms conventional techniques by the orders of magnitude in means of reflection coefficients and can be placed extremely close to any scatterers. Berenger first proposed a split-field formulation, where by choosing the suitable parameters, a perfectly matched planar interface between the PML medium and the modeled region is acquired [8, 9]. Later, this concept has been restated in a stretched-coordinate form by Chew [10]. Based on a Maxwellian formulation rather than a mathematical model, an uniaxial anisotropic medium with both magnetic and electric permittivity tensors was applied in the FDTD simulations [11]. It does not need split the fields and results in similar performance with the Berenger's counterpart. Recently, both the PMLs have been used in the finite-element method [12], TLM [13], and computational acoustics [14] as absorbing boundary conditions. However, in the discrete space, the electric and magnetic parameters are represented in piecewise and spatially staggered manners, consequently, spurious reflections were produced from discretization, material discontinuities. Both PMLs can achieve reflectionless truncations only in the continuum limit as mesh size goes to zero. Some theoretical analyses were made to improve their performance based on two-dimensional Berenger's PMLs [15], however, no effort was made on three-dimensional Berenger's and two- and three-dimensional uniaxial PMLs mechanism behind their performance.

This paper specially focuses on the investigations on both three-dimensional Berenger's and uniaxial perfectly matched layers in the discrete space, and their numerical dispersion and impedance are rigorously analyzed, respectively. The investigations provide

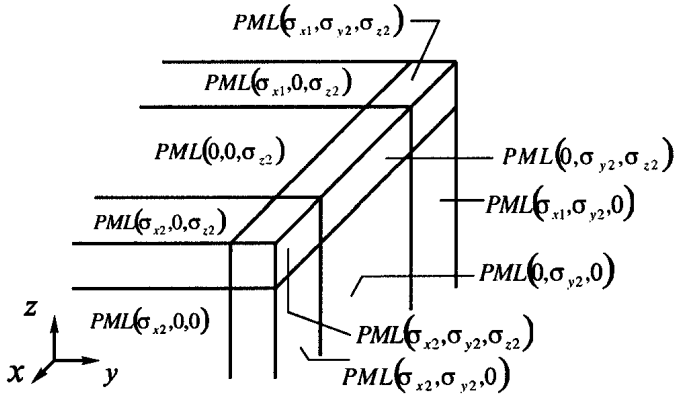

Figure 1. Upper-right part of computational domain surrounded by the PML layers.

theoretical support to understand their impact on the absorbing performance and design the most efficient three-dimensional PMLs. This paper is organized as follows: the Section 2 briefly describes the methodologies, numerical characteristics of three-dimensional Berenger's and uniaxial perfectly matched layers are analyzed respectively in the Sections 3 and 4, and the last section draws the conclusions.

2. THE PERFECTLY MATCHED LAYERS' FORMULATIONS

For solving an unbounded problem using the FDTD method, the perfectly matched layers are usually used as an absorbing material surrounding the modeled regions, as shown in Fig. 1. Herein, two types of PML methods are presented, namely, Berenger's PML and uniaxial PML.

2.1. The Berenger's PML

In the Berenger's PML medium, the electromagnetic field components are split into sub-components where, in the Cartesian Coordinates system, x sub-components of the electric and magnetic fields are satisfied with the following equations;

$$\varepsilon\frac{\partial E_{xy}}{\partial t}+\sigma_y E_{xy}=\frac{\partial H_z}{\partial y},\qquad \varepsilon\frac{\partial E_{xz}}{\partial t}+\sigma_z E_{xz}=-\frac{\partial H_y}{\partial z} \tag{1a}$$

$$\mu\frac{\partial H_{xy}}{\partial t} + \sigma_y^* H_{xy} = -\frac{\partial E_z}{\partial y}, \quad \mu\frac{\partial H_{xz}}{\partial t} + \sigma_z^* H_{xz} = \frac{\partial E_y}{\partial z} \tag{1b}$$

where

$$E_x = E_{xy} + E_{xz}, \qquad H_x = H_{xy} + H_{xz} \tag{2}$$

and the other sub-components have the similar formulations. If the conductivities are satisfied with the following matched-impedance condition;

$$\sigma_i/\varepsilon = \sigma_i^*/\mu \quad i = x, y, z \tag{3}$$

where σ, σ^* is the electrical and magnetic conductivities and ε, μ are the permittivity and permeability of the corresponding media in the PML region and the modeled region as set in Fig. 1. Theoretically, the electromagnetic wave with arbitrary polarization, frequency, and incidence from the modeled region impinges on the PML medium without reflection and gradually diminishes as traveling into the PML material, hence it is effectively absorbed. The finite-difference implementations for Eq. (1a) using exponential finite-difference approximation are given as;

$$E_{xy}^{n+1}(i+1/2, j, k) = Ae_y(j)E_{xy}^n(i+1/2, j, k) - Be_y(j) \\ [H_z(i+1/2, j+1/2, k) - H_z(i+1/2, j-1/2, k)]^{n+1/2}/\Delta y(j) \tag{4a}$$

$$E_{xz}^{n+1}(i+1/2, j, k) = Ae_z(k)E_{xz}^n(i+1/2, j, k) - Be_z(k) \\ [H_y(i+1/2, j, k-1/2) - H_y(i+1/2, j, k+1/2)]^{n+1/2}/\Delta z(k) \tag{4b}$$

where

$$Ae_i(l) = \exp[-(\sigma_i(l)\Delta t)/\varepsilon] \tag{5a}$$

$$Be_i(l) = \{\exp[-(\sigma_i(l)\Delta t)/\varepsilon] - 1\}/\sigma_i(l) \tag{5b}$$

2.2. The Uniaxial PML

The uniaxial perfectly matched layer medium is anisotropic and composed of both electric and magnetic permittivity tensors for a single interface, where the electromagnetic fields are satisfied to the following equations;

$$\nabla \times \vec{E} = \frac{\partial}{\partial t}\begin{bmatrix} \kappa_y & 0 & 0 \\ 0 & \kappa_z & 0 \\ 0 & 0 & \kappa_x \end{bmatrix}\vec{B} - \frac{1}{\varepsilon_0}\begin{bmatrix} \sigma_y & 0 & 0 \\ 0 & \sigma_z & 0 \\ 0 & 0 & \sigma_x \end{bmatrix}\vec{B} \tag{6a}$$

$$\frac{\partial}{\partial t}\begin{bmatrix}\kappa_x & 0 & 0\\ 0 & \kappa_y & 0\\ 0 & 0 & \kappa_z\end{bmatrix}\vec{B}+\frac{1}{\varepsilon_0}\begin{bmatrix}\sigma_x & 0 & 0\\ 0 & \sigma_y & 0\\ 0 & 0 & \sigma_z\end{bmatrix}\vec{B}$$
$$=\mu\frac{\partial}{\partial t}\begin{bmatrix}\kappa_z & 0 & 0\\ 0 & \kappa_x & 0\\ 0 & 0 & \kappa_y\end{bmatrix}\vec{H}+\frac{\mu}{\varepsilon_0}\begin{bmatrix}\sigma_z & 0 & 0\\ 0 & \sigma_x & 0\\ 0 & 0 & \sigma_y\end{bmatrix}\vec{H} \tag{6b}$$

$$\nabla\times\vec{H}=\frac{\partial}{\partial t}\begin{bmatrix}\kappa_y & 0 & 0\\ 0 & \kappa_z & 0\\ 0 & 0 & \kappa_x\end{bmatrix}\vec{D}+\frac{1}{\varepsilon_0}\begin{bmatrix}\sigma_y & 0 & 0\\ 0 & \sigma_z & 0\\ 0 & 0 & \sigma_x\end{bmatrix}\vec{D} \tag{7a}$$

$$\frac{\partial}{\partial t}\begin{bmatrix}\kappa_x & 0 & 0\\ 0 & \kappa_y & 0\\ 0 & 0 & \kappa_z\end{bmatrix}\vec{D}+\frac{1}{\varepsilon_0}\begin{bmatrix}\sigma_x & 0 & 0\\ 0 & \sigma_y & 0\\ 0 & 0 & \sigma_z\end{bmatrix}\vec{D}$$
$$=\varepsilon\frac{\partial}{\partial t}\begin{bmatrix}\kappa_z & 0 & 0\\ 0 & \kappa_x & 0\\ 0 & 0 & \kappa_y\end{bmatrix}\vec{E}+\frac{\varepsilon}{\varepsilon_0}\begin{bmatrix}\sigma_z & 0 & 0\\ 0 & \sigma_x & 0\\ 0 & 0 & \sigma_y\end{bmatrix}\vec{E} \tag{7b}$$

If $\kappa_i=1,\ \sigma_i=0,\ i=x,y,z$, Eqs. (6) and (7) are reduced to Maxwell's equations in the normal lossless medium. When this medium truncates the modeled region with the interface with the normal of $\hat{z}$, and $\sigma_x=\sigma_y=0$, the similar performance with the Berenger's PML medium can be acquired. The finite-difference implementations of x-components in Eqs. (6) and (7) by using central difference approximation are given as;

$$D_x\Big|_{i+\frac{1}{2},j,k}^{n+\frac{1}{2}}=\chi_y D_x\Big|_{i+\frac{1}{2},j,k}^{n-\frac{1}{2}}$$
$$+\zeta_y\left(\frac{H_z\Big|_{i+\frac{1}{2},j+\frac{1}{2},k}^{n}-H_z\Big|_{i+\frac{1}{2},j-\frac{1}{2},k}^{n}}{\Delta y}-\frac{H_y\Big|_{i+\frac{1}{2},j,k+\frac{1}{2}}^{n}-H_y\Big|_{i+\frac{1}{2},j,k-\frac{1}{2}}^{n}}{\Delta z}\right) \tag{8a}$$

$$E_x\Big|_{i+\frac{1}{2},j,k}^{n+\frac{1}{2}}=\chi_z E_x\Big|_{i+\frac{1}{2},j,k}^{n-\frac{1}{2}}+\frac{\zeta_z}{\varepsilon\zeta_x}\left[D_x\Big|_{i+\frac{1}{2},j,k}^{n+\frac{1}{2}}-\chi_x D_x\Big|_{i+\frac{1}{2},j,k}^{n-\frac{1}{2}}\right] \tag{8b}$$

$$B_x\Big|_{i,j+\frac{1}{2},k+\frac{1}{2}}^{n+1}=\chi_y B_x\Big|_{i,j+\frac{1}{2},k+\frac{1}{2}}^{n}$$
$$-\zeta_y\left(\frac{E_z\Big|_{i,j+1,k+\frac{1}{2}}^{n+\frac{1}{2}}-E_z\Big|_{i,j,k+\frac{1}{2}}^{n+\frac{1}{2}}}{\Delta y}-\frac{E_y\Big|_{i,j+\frac{1}{2},k+1}^{n+\frac{1}{2}}-E_y\Big|_{i,j+\frac{1}{2},k}^{n+\frac{1}{2}}}{\Delta z}\right) \tag{8c}$$

$$H_x\Big|_{i,j+\frac{1}{2},k+\frac{1}{2}}^{n+1} = \chi_z H_x\Big|_{i,j+\frac{1}{2},k+\frac{1}{2}}^{n} + \frac{\zeta_z}{\mu\zeta_x}\left[B_x\Big|_{i,j+\frac{1}{2},k+\frac{1}{2}}^{n+1} - \chi_x B_x\Big|_{i,j+\frac{1}{2},k+\frac{1}{2}}^{n}\right] \tag{8d}$$

where

$$\chi_\tau = \frac{\dfrac{\kappa_\tau}{\Delta t} - \dfrac{\sigma_\tau}{2\varepsilon_0}}{\dfrac{\kappa_\tau}{\Delta t} + \dfrac{\sigma_\tau}{2\varepsilon_0}} \qquad \zeta_\tau = \frac{1}{\dfrac{\kappa_\tau}{\Delta t} + \dfrac{\sigma_\tau}{2\varepsilon_0}}, \qquad \tau = x, y, z \tag{9}$$

The finite-difference equations for the other components in Eqs. (6) and (7) can be acquired in the similar ways. Although the electromagnetic waves with arbitrary incidence and frequency from the modeled region can effectively enter into and be attenuated within both PML media, the reflection is still produced as a perfect electric conductor is placed at the outer boundaries of the PML media. For a plane wave, an apparent reflection is a function of PML's thickness and its conductivity as expressed in the following equation;

$$|\Gamma_{PML}| = e^{-(2\cos\theta/\varepsilon_0\nu)\int_0^\delta \sigma_i(\rho)d\rho} \tag{10}$$

where δ, θ, ν is the thickness, angle of incidence, and the velocity of light in the PML medium, respectively. Theoretically, a PML with the reflection as small as required can be obtained by increasing PML's thickness or conductivity or both. Unfortunately, such an achievement cannot be obtained for any perfectly matched layers in the discrete space because Eq. (10) does not take account of the contribution of conductivity's variation, discretization, and the field placement in the FDTD cell.

3. NUMERICAL CHARACTERISTICS OF 3D BERENGER'S PML

3.1. Numerical Dispersion

To analyze numerical dispersion in three-dimensional Berenger's PML medium, it is assumed that the medium is homogeneous and the plane harmonic waves governed by Eq. (11) are propagated there;

$$\psi(x, y, z, t) = \psi_0 e^{j(\omega t - k_x x - k_y y - k_z z)} \tag{11}$$

where $\psi(x, y, z, t)$ is the sub-components of the electromagnetic fields with the amplitude of ψ_0 and k_x, k_y, k_z are wave numbers along x, y, z directions.

When Eq. (11) is substituted into the Berenger's PML's finite-difference equations, for example, into Eq. (4), the following equation is acquired;

$$E_{x0} = \frac{Be_y \times 2j\sin(k_y\Delta y/2)}{\Delta y\left[e^{j\omega\Delta t/2} - Ae_y e^{-j\omega\Delta t/2}\right]} H_{z0} - \frac{Be_z \times 2j\sin(k_z\Delta z/2)}{\Delta z\left[e^{j\omega\Delta t/2} - Ae_z e^{-j\omega\Delta t/2}\right]} H_{y0} \tag{12}$$

where all the FDTD cells are supposed to be uniform. The other five equations for the rest components of the electromagnetic fields can be achieved in the same way, and a system of linear equations are written as;

$$\Lambda\Re = 0 \tag{13}$$

where

$$\Lambda = \begin{bmatrix} 1 & 0 & 0 & 0 & \xi_z & -\xi_y \\ 0 & 1 & 0 & -\xi_z & 0 & \xi_x \\ 0 & 0 & 1 & \xi_y & -\xi_x & 0 \\ 0 & -\vartheta_z & \vartheta_y & 1 & 0 & 0 \\ \vartheta_z & 0 & -\vartheta_x & 0 & 1 & 0 \\ -\vartheta_y & \vartheta_x & 0 & 0 & 0 & 1 \end{bmatrix} \qquad \Re = \begin{bmatrix} E_{x0} \\ E_{y0} \\ E_{z0} \\ H_{x0} \\ H_{y0} \\ H_{z0} \end{bmatrix} \tag{14}$$

$$\begin{aligned} \xi_x &= [Be_x \times 2j\sin(k_x\Delta x/2)]/\left[\Delta x\left(e^{j\omega\Delta t/2} - Ae_x e^{-j\omega\Delta t/2}\right)\right] \\ \xi_y &= [Be_y \times 2j\sin(k_y\Delta y/2)]/\left[\Delta y\left(e^{j\omega\Delta t/2} - Ae_y e^{-j\omega\Delta t/2}\right)\right] \\ \xi_z &= [Be_z \times 2j\sin(k_z\Delta z/2)]/\left[\Delta z\left(e^{j\omega\Delta t/2} - Ae_z e^{-j\omega\Delta t/2}\right)\right] \end{aligned} \tag{15a}$$

$$\begin{aligned} \vartheta_x &= [Bh_x \times 2j\sin(k_x\Delta x/2)]/\left[\Delta x\left(e^{j\omega\Delta t/2} - Ah_x e^{-j\omega\Delta t/2}\right)\right] \\ \vartheta_y &= [Bh_y \times 2j\sin(k_y\Delta y/2)]/\left[\Delta y\left(e^{j\omega\Delta t/2} - Ah_y e^{-j\omega\Delta t/2}\right)\right] \\ \vartheta_z &= [Bh_z \times 2j\sin(k_z\Delta z/2)]/\left[\Delta z\left(e^{j\omega\Delta t/2} - Ah_z e^{-j\omega\Delta t/2}\right)\right] \end{aligned} \tag{15b}$$

and $E_{x0}, \ldots, H_{z0}$ are the amplitudes of the corresponding electromagnetic fields. If Eq. (13) has the non-zero solution, the following condition must be satisfied;

$$|\Lambda| = 0 \tag{16}$$

That is,

$$\xi_x\vartheta_x + \xi_y\vartheta_y + \xi_z\vartheta_z = 1 \tag{17}$$

Using the matched-impedance condition, Eq. (3), the numerical dispersion of three-dimensional Berenger's PMLs in the discrete space is derived as follows:

$$\frac{\sin^2[(k_x\Delta x)/2]}{\Delta x^2}G^2 + \frac{\sin^2[(k_y\Delta y)/2]}{\Delta y^2}H^2 + \frac{\sin^2[(k_z\Delta z)/2]}{\Delta z^2}R^2 = \frac{\sin^2[(\omega\Delta t)/2]}{(c\Delta t)^2} \tag{18}$$

where

$$\begin{aligned} G &= \frac{\varepsilon[\exp(-\sigma_x\Delta t/\varepsilon)-1](e^{j\omega\Delta t}-1)}{\Delta t\sigma_x[e^{j\omega\Delta t}-\exp(-\sigma_x\Delta t/\varepsilon)]} \\ H &= \frac{\varepsilon[\exp(-\sigma_y\Delta t/\varepsilon)-1](e^{j\omega\Delta t}-1)}{\Delta t\sigma_y[e^{j\omega\Delta t}-\exp(-\sigma_y\Delta t/\varepsilon)]} \\ R &= \frac{\varepsilon[\exp(-\sigma_z\Delta t/\varepsilon)-1](e^{j\omega\Delta t}-1)}{\Delta t\sigma_z[e^{j\omega\Delta t}-\exp(-\sigma_z\Delta t/\varepsilon)]} \end{aligned} \tag{19}$$

In the practical applications, for example, three-dimensional PML truncating the modeled region with the interface with the normal of $\hat{z}$ needs $\sigma_x, \sigma_y \to 0$ according to the conditions of the Berenger's PML, hence, the numerical dispersion in this planar Berenger's PML is given by;

$$\frac{\sin^2[(k_x\Delta x)/2]}{\Delta x^2} + \frac{\sin^2[(k_y\Delta y)/2]}{\Delta y^2} + \frac{\sin^2[(k_z\Delta z)/2]}{\Delta z^2}R^2 = \frac{\sin^2[(\omega\Delta t)/2]}{(c\Delta t)^2} \tag{20}$$

In two-dimensional Berenger's PML using the x-z plane, Eq. (20) is reduced to;

$$\frac{\sin^2[(k_x\Delta x)/2]}{\Delta x^2} + \frac{\sin^2[(k_z\Delta z)/2]}{\Delta z^2}R^2 = \frac{\sin^2[(\omega\Delta t)/2]}{(c\Delta t)^2} \tag{21}$$

If this medium becomes lossless, that is, $\sigma_x = \sigma_x^* = \sigma_y = \sigma_y^* = \sigma_z = \sigma_z^* = 0$, the numerical dispersion in this medium is obtained as follows;

$$\frac{\sin^2[(k_x\Delta x)/2]}{\Delta x^2} + \frac{\sin^2[(k_y\Delta y)/2]}{\Delta y^2} + \frac{\sin^2[(k_z\Delta z)/2]}{\Delta z^2} = \frac{\sin^2[(\omega\Delta t)/2]}{(c\Delta t)^2} \tag{22}$$

Equation (22) is the numerical dispersion satisfied by the finite-difference time-domain equations in any lossless medium. If $\Delta t \to$

0, $\Delta x \to 0$, $\Delta y \to 0$, and $\Delta z \to 0$, Eq. (18) becomes;

$$k_x^2 \left(\frac{j\omega\varepsilon}{j\omega\varepsilon + \sigma_x} \right)^2 + k_y^2 \left(\frac{j\omega\varepsilon}{j\omega\varepsilon + \sigma_y} \right)^2 + k_z^2 \left(\frac{j\omega\varepsilon}{j\omega\varepsilon + \sigma_z} \right)^2 = k^2 \quad (23)$$

It is the dispersion relationship of the differential equations satisfied by the fields in the Berenger's PML medium, where k is the wave number.

The numerical dispersion in one-dimensional homogeneous PML medium in the discrete space is;

$$\frac{\sin(k\Delta x/2)}{\Delta x} G = \frac{\sin(\omega\Delta t/2)}{c\Delta t} \quad (24)$$

where

$$G = \frac{\varepsilon_0[\exp(-\sigma\Delta t/\varepsilon_0) - 1](e^{j\omega\Delta t} - 1)}{\Delta t\sigma[e^{j\omega\Delta t} - \exp(-\sigma\Delta t/\varepsilon_0)]} \quad (25)$$

When $c\Delta t/\Delta x = 0.5$, $\Delta x/\lambda = 0.05$, and $f = 15\,\mathrm{GHz}$, the change of propagation constant with electric conductivity is shown in Fig. 2, which is normalized by the wave number in free space. When $c\Delta t/\Delta x = 0.5$ and $\sigma = 2\,\mathrm{S/m}$, the change of normalized propagation constant with the frequency is shown in Fig. 3. It can be found that the attenuation increases with conductivity, whilst phase constant remains unchanged in a wide range of frequency in the discrete space if the conductivities are chosen correctly.

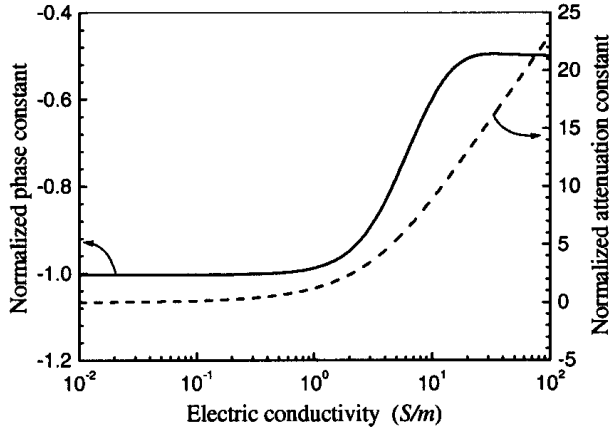

Figure 2. The change of propagation constant with the electric conductivity in the PML medium.

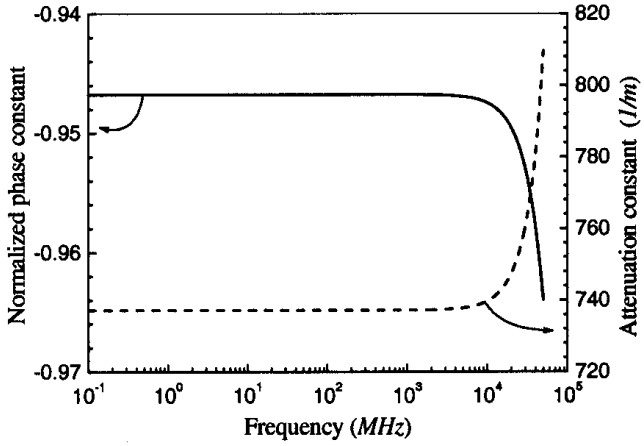

Figure 3. The change of propagation constant with the frequency in the PML medium.

3.2. Impedance

The impedance in the perfectly matched layer medium, which can interpret its absorbing performance, can be defined in the various ways. Since it represents the ratio between the electric and magnetic fields, the following equations are defined for the fields within any medium;

$$\begin{aligned} Z_{xy} &= E_x/H_y, \qquad Z_{xz} = E_x/H_z \\ Z_{yx} &= E_y/H_x, \qquad Z_{yz} = E_y/H_z \\ Z_{zx} &= E_z/H_x, \qquad Z_{zy} = E_z/H_y \end{aligned} \tag{26}$$

A system of nonlinear equations are obtained through the reconstruction of Eq. (13);

$$\begin{cases} Z_{xy}Z_{xz} - \xi_y Z_{xy} + \xi_z Z_{xz} = 0 \\ Z_{yx}Z_{yz} + \xi_x Z_{yx} - \xi_z Z_{yz} = 0 \\ Z_{zx}Z_{zy} - \xi_x Z_{zx} + \xi_y Z_{zy} = 0 \\ 1 + \vartheta_y Z_{zx} - \vartheta_z Z_{yx} = 0 \\ 1 + \vartheta_z Z_{xy} - \vartheta_x Z_{zy} = 0 \\ 1 + \vartheta_x Z_{yz} - \vartheta_y Z_{xz} = 0 \end{cases} \tag{27}$$

The solutions for Eq. (27) are;

$$\begin{cases} Z_{xy} = \frac{-\xi_x\vartheta_x-\xi_y\vartheta_y+\xi_z\vartheta_z+1\pm\sqrt{(\xi_x\vartheta_x+\xi_y\vartheta_y+\xi_z\vartheta_z-1)^2-4\xi_x\xi_y\xi_z\vartheta_x\vartheta_y\vartheta_z}}{2\vartheta_z(\xi_y\vartheta_y-1)} \\ Z_{xz} = \frac{\xi_x\vartheta_x-\xi_y\vartheta_y+\xi_z\vartheta_z-1\pm\sqrt{(\xi_x\vartheta_x+\xi_y\vartheta_y+\xi_z\vartheta_z-1)^2-4\xi_x\xi_y\xi_z\vartheta_x\vartheta_y\vartheta_z}}{2\vartheta_y(\xi_z\vartheta_z-1)} \\ Z_{yx} = \frac{\xi_x\vartheta_x+\xi_y\vartheta_y-\xi_z\vartheta_z-1\pm\sqrt{(\xi_x\vartheta_x+\xi_y\vartheta_y+\xi_z\vartheta_z-1)^2-4\xi_x\xi_y\xi_z\vartheta_x\vartheta_y\vartheta_z}}{2\vartheta_z(\xi_x\vartheta_x-1)} \\ Z_{yz} = \frac{\xi_x\vartheta_x-\xi_y\vartheta_y-\xi_z\vartheta_z+1\pm\sqrt{(\xi_x\vartheta_x+\xi_y\vartheta_y+\xi_z\vartheta_z-1)^2-4\xi_x\xi_y\xi_z\vartheta_x\vartheta_y\vartheta_z}}{2\vartheta_x(\xi_z\vartheta_z-1)} \\ Z_{zx} = \frac{-\xi_x\vartheta_x+\xi_y\vartheta_y-\xi_z\vartheta_z+1\pm\sqrt{(\xi_x\vartheta_x+\xi_y\vartheta_y+\xi_z\vartheta_z-1)^2-4\xi_x\xi_y\xi_z\vartheta_x\vartheta_y\vartheta_z}}{2\vartheta_y(\xi_x\vartheta_x-1)} \\ Z_{zy} = \frac{-\xi_x\vartheta_x+\xi_y\vartheta_y+\xi_z\vartheta_z-1\pm\sqrt{(\xi_x\vartheta_x+\xi_y\vartheta_y+\xi_z\vartheta_z-1)^2-4\xi_x\xi_y\xi_z\vartheta_x\vartheta_y\vartheta_z}}{2\vartheta_x(\xi_y\vartheta_y-1)} \end{cases} \tag{28}$$

They are the impedance relationship in three-dimensional lossy anisotropic medium in the discrete space. Using the numerical dispersion Eq. (17) and the matched-impedance condition Eq. (3), Eq. (28) becomes;

$$\begin{aligned} Z_{xy} &= \eta\frac{\xi_z\eta \pm j\xi_x\xi_y}{\xi_y^2-\eta^2} \qquad Z_{xz} = \eta\frac{-\xi_y\eta \pm j\xi_x\xi_z}{\xi_z^2-\eta^2} \\ Z_{yx} &= \eta\frac{-\xi_z\eta \pm j\xi_x\xi_y}{\xi_x^2-\eta^2} \qquad Z_{yz} = \eta\frac{\xi_x\eta \pm j\xi_y\xi_z}{\xi_z^2-\eta^2} \\ Z_{zx} &= \eta\frac{\xi_y\eta \pm j\xi_x\xi_z}{\xi_x^2-\eta^2} \qquad Z_{zy} = \eta\frac{-\xi_x\eta \pm j\xi_y\xi_z}{\xi_y^2-\eta^2} \end{aligned} \tag{29}$$

It is the impedance relationship in three-dimensional lossy medium satisfying with the matched-impedance condition in the discrete space. Suppose that this lossy medium locates on $z \geq 0$, $\sigma_x = \sigma_y = 0$ holds true for the Berenger's perfectly matched layers. Assume that the fields within the PML region are part of a plane wave traveling from the truncated region into the perfectly matched layers. It is observed from FDTD and PML time-stepping equations that the field dependence in the transverse (to the boundary) directions for the plane wave in both regions are identical, hence $k_{xp} = k_{xf}$, $k_{yp} = k_{yf}$, where k_{xp}, k_{yp} are propagation constant along x, y directions in PML medium and k_{xf}, k_{yf} are those in the truncated medium, respectively. By using those conditions and numerical dispersion in both media Eqs. (20) and (22), the following equation is obtained;

$$\frac{\sin[(k_{zp}\Delta z)/2]}{\Delta z}R = \pm\frac{\sin[(k_{zf}\Delta z)/2]}{\Delta z} \tag{30}$$

and the parameters in the PML medium can be expressed as follows

$$\begin{aligned}
\xi_x &= -\eta\frac{\nu\Delta t}{\Delta x}\frac{\sin[(k_{xf}\Delta x)/2]}{\sin[(\omega\Delta t)/2]} \\
\xi_y &= -\eta\frac{\nu\Delta t}{\Delta y}\frac{\sin[(k_{yf}\Delta y)/2]}{\sin[(\omega\Delta t)/2]} \\
\xi_z &= \pm\eta\frac{\nu\Delta t}{\Delta z}\frac{\sin[(k_{zf}\Delta z)/2]}{\sin[(\omega\Delta t)/2]}
\end{aligned} \tag{31}$$

The impedance in three-dimensional homogeneous Berenger's PML medium with the interface with the normal of $\hat{z}$ in the discrete space is obtained through the substitution of Eq. (31) into Eq. (29). It can be found that it is the same as one in the truncated normal medium even in the discrete space at any frequency and incidence, which theoretically leads to the penetration of the outgoing wave into the Berenger's PML medium without reflection. However, in the practical applications, because of the material's inhomogeneity near the interface, the PML medium is deviated from matched-impedance situation, which is the reason that the Berenger's PML is theoretically perfect, but still reflects the electromagnetic waves in numerical implementation. In two-dimensional case using the x-z plane, where only E_y, H_x, H_z need be considered for TM^y, Eq. (29) is degraded to;

$$\begin{cases}
Z_{yx} = \dfrac{-\xi_z\eta^2}{\xi_x^2 - \eta^2} \\
Z_{yz} = \dfrac{\xi_x\eta^2}{\xi_z^2 - \eta^2}
\end{cases} \tag{32}$$

If the PML medium locates in $z \geq 0$, according to $k_{xp} = k_{xf}$ with the same reason as before and numerical dispersion in both media, respectively, the following equations are obtained;

$$\begin{aligned}
\xi_x &= -\frac{\Delta t}{\varepsilon\Delta x}\frac{\sin[(k_{xp}\Delta x)/2]}{\sin[(\omega\Delta t)/2]} = -\frac{\Delta t}{\varepsilon\Delta x}\frac{\sin[(k_{xf}\Delta x)/2]}{\sin[(\omega\Delta t)/2]} \\
\xi_z &= \frac{e^{-(\sigma_z\Delta t)/\varepsilon} - 1}{\sigma_z\Delta z}\frac{2j\sin[(k_{zp}\Delta z)/2]}{e^{j\omega\Delta t/2} - e^{-(\sigma_z\Delta t)/\varepsilon}e^{-j\omega\Delta t/2}} \\
&= \pm\frac{\Delta t}{\varepsilon\Delta z}\frac{\sin[(k_{zf}\Delta z)/2]}{\sin[(\omega\Delta t)/2]}
\end{aligned} \tag{33}$$

Hence, the impedance in homogeneous PML for two-dimensional TM^y case is;

$$\begin{aligned} Z_{yx} &= \pm\frac{\mu\Delta z}{\Delta t}\frac{\sin[(\omega\Delta t)/2]}{\sin[(k_{zf}\Delta z)/2]} \\ Z_{yz} &= \frac{\mu\Delta x}{\Delta t}\frac{\sin[(\omega\Delta t)/2]}{\sin[(k_{xf}\Delta x)/2]} \end{aligned} \tag{34}$$

This impedance is the same as that in the truncated normal medium.

4. NUMERICAL CHARACTERISTICS OF 3D UNIAXIAL PML

4.1. Numerical Dispersion

When a harmonic plane electromagnetic wave is propagated in the uniaxial perfectly matched layer medium where any components of the electromagnetic fields $\vec{E}, \vec{D}, \vec{B}, \vec{H}$ have the form of Eq. (11), the following system of the equations are acquired through the substitution of Eq. (11) into Eq. (8) as follows;

$$\aleph\Re = 0 \tag{35}$$

where

$$\aleph = \begin{bmatrix} 1 & 0 & 0 & 0 & -\frac{\wp_x\hbar_z}{\varepsilon} & \frac{\wp_x\hbar_y}{\varepsilon} \\ 0 & 1 & 0 & \frac{\wp_y\hbar_z}{\varepsilon} & 0 & -\frac{\wp_y\hbar_x}{\varepsilon} \\ 0 & 0 & 1 & -\frac{\wp_z\hbar_y}{\varepsilon} & \frac{\wp_z\hbar_x}{\varepsilon} & 0 \\ 0 & \frac{\wp_x\hbar_z}{\mu} & -\frac{\wp_x\hbar_y}{\mu} & 1 & 0 & 0 \\ -\frac{\wp_y\hbar_z}{\mu} & 0 & \frac{\wp_y\hbar_x}{\mu} & 0 & 1 & 0 \\ \frac{\wp_z\hbar_y}{\mu} & -\frac{\wp_z\hbar_x}{\mu} & 0 & 0 & 0 & 1 \end{bmatrix} \quad \Re = \begin{bmatrix} E_{x0} \\ E_{y0} \\ E_{z0} \\ H_{x0} \\ H_{y0} \\ H_{z0} \end{bmatrix} \tag{36}$$

$$\wp_x = \frac{\zeta_y\zeta_z(1-\chi_x e^{-j\omega\Delta t})e^{-j\omega\Delta t/2}}{\zeta_x(1-\chi_y e^{-j\omega\Delta t})(1-\chi_z e^{-j\omega\Delta t})} \quad \hbar_x = \frac{j2\sin(k_x\Delta x/2)}{\Delta x} \tag{37a}$$

$$\wp_y = \frac{\zeta_x\zeta_z(1-\chi_y e^{-j\omega\Delta t})e^{-j\omega\Delta t/2}}{\zeta_y(1-\chi_x e^{-j\omega\Delta t})(1-\chi_z e^{-j\omega\Delta t})} \quad \hbar_y = \frac{j2\sin(k_y\Delta y/2)}{\Delta y} \tag{37b}$$

$$\wp_z = \frac{\zeta_x\zeta_y(1-\chi_z e^{-j\omega\Delta t})e^{-j\omega\Delta t/2}}{\zeta_z(1-\chi_x e^{-j\omega\Delta t})(1-\chi_y e^{-j\omega\Delta t})} \quad \hbar_z = \frac{j2\sin(k_z\Delta z/2)}{\Delta z} \tag{37c}$$

The condition leading to a nonzero solution for Eq. (35) is;

$$|\aleph| = 0 \tag{38}$$

This makes the following equation hold true;

$$\wp_y\wp_z\hbar_x^2 + \wp_x\wp_z\hbar_y^2 + \wp_x\wp_y\hbar_z^2 = \varepsilon\mu \tag{39}$$

or

$$\frac{\zeta_x^2 e^{-j\omega\Delta t}}{(1-\chi_x e^{-j\omega\Delta t})^2}\hbar_x^2 + \frac{\zeta_y^2 e^{-j\omega\Delta t}}{(1-\chi_y e^{-j\omega\Delta t})^2}\hbar_y^2 + \frac{\zeta_z^2 e^{-j\omega\Delta t}}{(1-\chi_z e^{-j\omega\Delta t})^2}\hbar_z^2 = \varepsilon\mu \tag{40}$$

It is numerical dispersion in the uniaxial perfectly matched layer medium located in the corners of the UPML. On the other hand, three-dimensional UPML truncating the modeled region with the interface with the normal of $\hat{z}$ needs $\kappa_x = \kappa_y = 1$ and $\sigma_x, \sigma_y \to 0$ according to the planar UPML conditions, hence, the numerical dispersion in this planar UPML medium is;

$$\frac{\sin^2(k_x\Delta x/2)}{\Delta x^2} + \frac{\sin^2(k_y\Delta y/2)}{\Delta y^2} + P^2\frac{\sin^2(k_z\Delta z/2)}{\Delta z^2} = \frac{\sin^2\left(\dfrac{\omega\Delta t}{2}\right)}{(\nu\Delta t)^2} \tag{41}$$

where $P = \frac{j2\zeta_z e^{-j\omega\Delta t/2}\sin(k_x\Delta x/2)}{\Delta t(1-\chi_z e^{-j\omega\Delta t})}$. When the UPML medium becomes a lossless normal one, $\chi_\tau = 1$ and $\zeta_\tau = \Delta t$, then;

$$\frac{\sin^2\left(\dfrac{k_x\Delta x}{2}\right)}{\Delta x^2} + \frac{\sin^2\left(\dfrac{k_y\Delta y}{2}\right)}{\Delta y^2} + \frac{\sin^2\left(\dfrac{k_z\Delta z}{2}\right)}{\Delta z^2} = \frac{\sin^2\left(\dfrac{\omega\Delta t}{2}\right)}{(\nu\Delta t)^2} \tag{42}$$

This is numerical dispersion of the FDTD equations in the homogeneous lossless normal medium. When both the spatial and temporal discretization sizes tend to infinitesimal, Eq. (40) is reduced to dispersion relationship of the differential equations satisfied by the fields within the UPML medium;

$$\left(\frac{j\omega\varepsilon_0}{j\omega\varepsilon_0\kappa_x + \sigma_x}\right)^2 k_x^2 + \left(\frac{j\omega\varepsilon_0}{j\omega\varepsilon_0\kappa_y + \sigma_y}\right)^2 k_y^2 + \left(\frac{j\omega\varepsilon_0}{j\omega\varepsilon_0\kappa_z + \sigma_z}\right)^2 k_z^2 = k_0^2 \tag{43}$$

4.2. Impedance

When the impedance in the UPML medium is defined as Eq. (26), a system of nonlinear equations for the impedance can be derived as follows through the reconstruction of Eq. (35);

$$\begin{aligned}
Z_{xy}Z_{xz} + \frac{\wp_x\hbar_y}{\varepsilon}Z_{xy} - \frac{\wp_x\hbar_z}{\varepsilon}Z_{xz} &= 0\\
Z_{yx}Z_{yz} + \frac{\wp_y\hbar_z}{\varepsilon}Z_{yz} - \frac{\wp_y\hbar_x}{\varepsilon}Z_{yx} &= 0\\
Z_{zx}Z_{zy} + \frac{\wp_z\hbar_x}{\varepsilon}Z_{zx} - \frac{\wp_z\hbar_y}{\varepsilon}Z_{zy} &= 0\\
1 - \frac{\wp_x\hbar_y}{\mu}Z_{zx} + \frac{\wp_x\hbar_z}{\mu}Z_{yx} &= 0\\
1 - \frac{\wp_y\hbar_z}{\mu}Z_{xy} + \frac{\wp_y\hbar_x}{\mu}Z_{zy} &= 0\\
1 - \frac{\wp_z\hbar_x}{\mu}Z_{yz} + \frac{\wp_z\hbar_y}{\mu}Z_{xz} &= 0
\end{aligned} \tag{44}$$

The solutions to this system of nonlinear equations, Eq. (44), are;

$$\begin{aligned}
Z_{xy} &= \\
&\frac{\varepsilon\mu(\lambda_x^2\hbar_x^2+\lambda_y^2\hbar_y^2-\lambda_z^2\hbar_z^2-\varepsilon\mu)\pm\sqrt{(\varepsilon\mu)^2(\lambda_x^2\hbar_x^2+\lambda_y^2\hbar_y^2+\lambda_z^2\hbar_z^2-\varepsilon\mu)^2-4\varepsilon\mu\lambda_x^2\lambda_y^2\lambda_z^2\hbar_x^2\hbar_y^2\hbar_z^2}}{2\varepsilon\wp_y\hbar_z(\lambda_y^2\hbar_y^2-\varepsilon\mu)}\\
Z_{yx} &= \\
&\frac{\varepsilon\mu(\lambda_z^2\hbar_z^2-\lambda_x^2\hbar_x^2-\lambda_y^2\hbar_y^2+\varepsilon\mu)\pm\sqrt{(\varepsilon\mu)^2(\lambda_x^2\hbar_x^2+\lambda_y^2\hbar_y^2+\lambda_z^2\hbar_z^2-\varepsilon\mu)^2-4\varepsilon\mu\lambda_x^2\lambda_y^2\lambda_z^2\hbar_x^2\hbar_y^2\hbar_z^2}}{2\varepsilon\wp_x\hbar_z(\lambda_x^2\hbar_x^2-\varepsilon\mu)}\\
Z_{zx} &= \\
&\frac{\varepsilon\mu(\lambda_x^2\hbar_x^2+\lambda_z^2\hbar_z^2-\lambda_y^2\hbar_y^2-\varepsilon\mu)\pm\sqrt{(\varepsilon\mu)^2(\lambda_x^2\hbar_x^2+\lambda_y^2\hbar_y^2+\lambda_z^2\hbar_z^2-\varepsilon\mu)^2-4\varepsilon\mu\lambda_x^2\lambda_y^2\lambda_z^2\hbar_x^2\hbar_y^2\hbar_z^2}}{2\varepsilon\wp_x\hbar_y(\lambda_x^2\hbar_x^2-\varepsilon\mu)}\\
Z_{zy} &= \\
&\frac{\varepsilon\mu(\lambda_x^2\hbar_x^2-\lambda_y^2\hbar_y^2-\lambda_z^2\hbar_z^2+\varepsilon\mu)\pm\sqrt{(\varepsilon\mu)^2(\lambda_x^2\hbar_x^2+\lambda_y^2\hbar_y^2+\lambda_z^2\hbar_z^2-\varepsilon\mu)^2-4\varepsilon\mu\lambda_x^2\lambda_y^2\lambda_z^2\hbar_x^2\hbar_y^2\hbar_z^2}}{2\varepsilon\wp_y\hbar_x(\lambda_y^2\hbar_y^2-\varepsilon\mu)}\\
Z_{yz} &= \\
&\frac{\varepsilon\mu(\lambda_y^2\hbar_y^2+\lambda_z^2\hbar_z^2-\lambda_x^2\hbar_x^2-\varepsilon\mu)\pm\sqrt{(\varepsilon\mu)^2(\lambda_x^2\hbar_x^2+\lambda_y^2\hbar_y^2+\lambda_z^2\hbar_z^2-\varepsilon\mu)^2-4\varepsilon\mu\lambda_x^2\lambda_y^2\lambda_z^2\hbar_x^2\hbar_y^2\hbar_z^2}}{2\varepsilon\wp_z\hbar_x(\lambda_z^2\hbar_z^2-\varepsilon\mu)}\\
Z_{xz} &= \\
&\frac{\varepsilon\mu(\lambda_y^2\hbar_y^2-\lambda_x^2\hbar_x^2-\lambda_z^2\hbar_z^2+\varepsilon\mu)\pm\sqrt{(\varepsilon\mu)^2(\lambda_x^2\hbar_x^2+\lambda_y^2\hbar_y^2+\lambda_z^2\hbar_z^2-\varepsilon\mu)^2-4\varepsilon\mu\lambda_x^2\lambda_y^2\lambda_z^2\hbar_x^2\hbar_y^2\hbar_z^2}}{2\varepsilon\wp_z\hbar_y(\lambda_z^2\hbar_z^2-\varepsilon\mu)}
\end{aligned} \tag{45}$$

where

$$\lambda_x = \frac{\zeta_x e^{-j\omega\Delta t/2}}{1-\chi_x e^{-j\omega\Delta t}}, \quad \lambda_y = \frac{\zeta_y e^{-j\omega\Delta t/2}}{1-\chi_y e^{-j\omega\Delta t}}, \quad \lambda_z = \frac{\zeta_z e^{-j\omega\Delta t/2}}{1-\chi_z e^{-j\omega\Delta t}} \tag{46}$$

Using numerical dispersion in the UPML medium Eq. (39) and the relations;

$$\wp_x = \frac{\lambda_y \lambda_z}{\lambda_x}, \quad \wp_y = \frac{\lambda_x \lambda_z}{\lambda_y}, \quad \wp_z = \frac{\lambda_x \lambda_y}{\lambda_z} \tag{47}$$

They are reduced as;

$$\begin{aligned}
Z_{xy} &= \eta \frac{-\nu\lambda_z\hbar_z \pm j\nu^2\lambda_x\lambda_y\hbar_x\hbar_y}{\frac{\lambda_x}{\lambda_y}\left(\nu^2\lambda_y^2\hbar_y^2 - 1\right)} \qquad Z_{xz} = \eta \frac{\nu\lambda_y\hbar_y \pm j\nu^2\lambda_x\lambda_z\hbar_x\hbar_z}{\frac{\lambda_x}{\lambda_z}\left(\nu^2\lambda_z^2\hbar_z^2 - 1\right)} \\
Z_{yz} &= \eta \frac{-\nu\lambda_x\hbar_x \pm j\nu^2\lambda_y\lambda_z\hbar_y\hbar_z}{\frac{\lambda_y}{\lambda_z}\left(\nu^2\lambda_z^2\hbar_z^2 - 1\right)} \qquad Z_{yx} = \eta \frac{\nu\lambda_z\hbar_z \pm j\nu^2\lambda_x\lambda_y\hbar_x\hbar_y}{\frac{\lambda_y}{\lambda_x}\left(\nu^2\lambda_x^2\hbar_x^2 - 1\right)} \\
Z_{zx} &= \eta \frac{-\nu\lambda_y\hbar_y \pm j\nu^2\lambda_x\lambda_z\hbar_x\hbar_z}{\frac{\lambda_z}{\lambda_x}\left(\nu^2\lambda_x^2\hbar_x^2 - 1\right)} \qquad Z_{zy} = \eta \frac{\nu\lambda_x\hbar_x \pm j\nu^2\lambda_y\lambda_z\hbar_y\hbar_z}{\frac{\lambda_z}{\lambda_y}\left(\nu^2\lambda_y^2\hbar_y^2 - 1\right)}
\end{aligned} \tag{48}$$

It is the impedance in the UPML medium where only the matched-impedance conditions are satisfied, that is, at the corner regions of the UPML medium. When applied to the truncation of the computational region at $z \geq 0$, $\sigma_x = \sigma_y = 0$, $\kappa_x = \kappa_y = 1$, $k_{xp} = k_{xf}$, $k_{yp} = k_{yf}$ hold true with the same reason as discussed in the last section, where $k_{xp}, k_{yp}, k_{xf}, k_{yf}$ have the same meanings as those in the last section. By using those conditions in combination with numerical dispersion in the UPML medium, Eq. (41), and in the truncated normal medium, Eq. (42), the following equations are obtained;

$$\begin{aligned}
\lambda_x\hbar_x &= \frac{\Delta t}{\Delta x}\frac{\sin[(k_{xf}\Delta x)/2]}{\sin[(\omega\Delta t)/2]} \\
\lambda_y\hbar_y &= \frac{\Delta t}{\Delta y}\frac{\sin[(k_{yf}\Delta y)/2]}{\sin[(\omega\Delta t)/2]} \\
\lambda_z\hbar_z &= \pm\frac{\Delta t}{\Delta z}\frac{\sin[(k_{zf}\Delta z)/2]}{\sin[(\omega\Delta t)/2]}
\end{aligned} \tag{49}$$

In the discrete space, the impedance in three-dimensional homogeneous UPML medium used to truncate the region with the interface with the normal of $\hat{z}$ is obtained through the substitution of Eq. (49) into Eq. (48), which can be found to have the following relations with those

in the truncated normal medium;

$$\frac{Z_{ij}\Big|_p}{Z_{ij}\Big|_f} = \frac{\lambda_i}{\lambda_j} \tag{50}$$

Equation (50) indicates that three-dimensional homogeneous UPML medium has not the same impedance as the truncated normal medium in the discrete space, but the impedance in UPML medium will smoothly change from those of the normal medium as the conductivities and the variable κ_z slowly change from $\sigma_z = 0$, $\kappa_z = 1$ at the interface to those at the outer boundary. This is the substantial reason that the UPML can effectively absorb the outgoing electromagnetic wave with any frequency and incidence as an absorbing boundary condition. In two-dimensional case using the x-z plane, where only the field components E_y, H_x, H_z for TM^y need be considered, Eq. (48) is degraded to;

$$\begin{aligned} Z_{yx} &= 2j \sin\left(\frac{\omega\Delta t}{2}\right) \lambda_x \eta \frac{\nu\lambda_z\hbar_z}{\Delta t\left(\nu^2\lambda_x^2\hbar_x^2 - 1\right)} \\ Z_{yz} &= 2j \sin\left(\frac{\omega\Delta t}{2}\right) \lambda_z \eta \frac{-\nu\lambda_x\hbar_x}{\Delta t\left(\nu^2\lambda_z^2\hbar_z^2 - 1\right)} \end{aligned} \tag{51}$$

If the UPML medium locates in $z \geq 0$, the following equations are obtained according to $k_{xp} = k_{xf}$ and numerical dispersion in the UPML medium and in the truncated normal lossless medium;

$$\begin{aligned} \lambda_x\hbar_x &= \frac{\Delta t}{\Delta x}\frac{\sin[(k_{xf}\Delta x)/2]}{\sin[(\omega\Delta t)/2]} \\ \lambda_z\hbar_z &= \pm\frac{\Delta t}{\Delta z}\frac{\sin[(k_{zf}\Delta z)/2]}{\sin[(\omega\Delta t)/2]} \end{aligned} \tag{52}$$

hence, the impedance relationship of the homogeneous UPML medium in two-dimensional TM^y case is;

$$\begin{aligned} Z_{yx} &= \pm\frac{\mu\Delta z}{\Delta t}\frac{\sin[(\omega\Delta t)/2]}{\sin[(k_{zf}\Delta z)/2]} \\ Z_{yz} &= 2j \sin\left(\frac{\omega\Delta t}{2}\right) \frac{\lambda_z}{\Delta t}\frac{\mu\Delta x}{\Delta t}\frac{\sin[(\omega\Delta t)/2]}{\sin[(k_{xf}\Delta x)/2]} \end{aligned} \tag{53}$$

Like three-dimensional results, the impedance Z_{yz} in the 2D UPML medium is different from that in the truncated normal lossless medium.

5. CONCLUSIONS

Three-dimensional Berenger's and uniaxial perfectly matched layers are investigated respectively in term of numerical dispersion and impedance characteristics in the paper. Numerical dispersion implies an exact knowledge of the relationships between the nodal fields in both space and time. They are different from that of the normal FDTD equations within both 3D PML media in the discrete space because of the introduction of lossness. When the conductivities in both PML media vanish, they are reduced to that of the normal FDTD equations. The same dispersion characteristic is also derived as that of the differential equations governing the fields in both PMLs when the spatial and temporal discretization sizes approach zero as a limit. Wave impedance analysis aids in understanding wave transmission from the truncated medium into a PML medium. The impedance within the 3D homogeneous Berenger's PML is the same as those within the truncated normal medium even in the discrete space, however, within the uniaxial perfectly matched layer medium, it does not hold true, but the difference between the impedances within both the UPML medium and the truncated normal medium smoothly changes as the parameters of the UPML medium slowly changes. Those numerical dispersion and impedance characteristics are physically essential that both the perfectly matched layers can effectively absorb the outgoing electromagnetic waves with arbitrary frequency, polarization, and incidence.

REFERENCES

1. Taflove, A., *Advances in Computational Electrodynamics, the Finite-Difference Time-Domain Method*, Artech House, 1998.
2. Mur, G., "Absorbing boundary conditions for the finite-difference approximation of the time-domain electromagnetic-field equations," *IEEE Trans. Electromagn. Compat.*, Vol. 23, 377–382, 1981.
3. Liao, Z. P., H. L. Wong, B. Yang, and Y. Yuan, "A transmitting boundary for transient wave analyses," *Scientia Sinica*, Vol. 27, 1063–1076, 1984.
4. Mei, K. K. and J. Fang, "Superabsorption — a method to improve absorbing boundary conditions," *IEEE Trans. Antennas Propagat.*, Vol. 40, 1001–1010, 1992.
5. Teixeira, F. L. and W. C. Chew, "Differential forms, metrics, and the reflectionless absorption of electromagnetic waves," *Journal of Electromagnetic Waves and Applications*, Vol. 13, 665–686, 1999.

6. Buksas, M. W., "Implementing the perfectly matched layer absorbing boundary condition with mimetic differencing schemes," *Progress In Electromagnetics Research*, Vol. 32, 383–411, 2001.
7. Li, L. W., P. S. Kooi, M. S. Leong, and S. T. Chew, "FDTD analysis of sidecoupled microstrip filter," *Journal of Electromagnetic Waves and Applications*, Vol. 14, 1533–1548, 2000.
8. Berenger, J., "A perfectly matched layer for the absorption of electromagnetic waves," *Journal of Computational Physics*, Vol. 114, 185–200, 1994.
9. Berenger, J., "Three dimensional perfectly matched layer for the absorption of electromagnetic waves," *Journal of Computational Physics*, Vol. 127, 363–379, 1996.
10. Chew, W. C. and W. H. Weedon, "A 3D perfectly matched medium from modified Maxwell's equations with stretched coordinates," *Microwave and Optical Technology Letters*, Vol. 7, 599–604, 1994.
11. Gedney, S. D., "An anisotropic perfectly matched layer absorbing medium for the truncation of FDTD lattices," *IEEE Trans. Antennas and Propagat.*, Vol. 44, 1630–1639, 1996.
12. Tang, J., K. D. Paulsen, and S. A. Haider, "Perfectly matched layer mesh terminations for nodal-based finite element methods in electromagnetic scattering," *IEEE Trans. Antennas and Propagat.*, Vol. 46, 507–516, 1998.
13. Pena, N. and M. M. Ney, "Absorbing boundary conditions using perfectly matched layer (PML) technique for three-dimensional TLM simulations," *IEEE Trans. Microwave Theory Tech.*, Vol. 45, 1749–1755, 1997.
14. Qi, Q. and T. L. Geers, "Evaluation of perfectly matched layer for computational acoustics," *Journal of Computational Physics*, Vol. 139, 166–183, 1998.
15. Prescott, D. T. and N. V. Shuley, "Reflection analysis of FDTD boundary conditions — Part II: Berenger's PML absorbing layers," *IEEE Trans. Microwave Theory Tech.*, Vol. 45, 1171–1178, 1997.

Weiliang Yuan received his B.Sc., M.Sc. and Ph.D. degrees, all in electrical engineering, from Xidian University, China, in 1993, 1996 and 1999 respectively. Since 1999, he has been a senior research engineer in the Computational Electromagnetics and Electronics Division, Institute of High Performance Computing, Singapore.

His main interests are in numerical techniques for computational electromagnetics, electromagnetic compatibility, and signal integrity analysis.

Erping Li received his Ph.D. degree from Sheffield Hallam University in 1992 in electrical engineering. He has taken various positions in research institute and companies. Since 2000, he has been a member of technical staff as well as R&D manager in the Division of Computational Electromagnetics and Electronics, Institute of High Performance Computing, Singapore. Dr. Li is a senior member of IEEE. He is an elected deputy chairman for IEEE EMC Society, Singapore Chapter. He has published over 40 papers in international journals or conferences. His research interests include electromagnetic compatibility, computational electromagnetics, and nano-technology.